AXIAL-POWER-DISTRIBUTION OPTIMIZATION IN THE TUNGSTEN WATER-MODERATED REACTOR

by Edward Lantz

Lewis Research Center

Cleveland, Ohio

NATIONAL AERONAUTICS AND SPACE ADMINISTRATION • WASHINGTON, D. C. • MAY 1966

[redacted]

AXIAL-POWER-DISTRIBUTION OPTIMIZATION IN THE TUNGSTEN WATER-MODERATED REACTOR

By Edward Lantz

Lewis Research Center
Cleveland, Ohio

[redacted]

ATOMIC ENERGY ACT OF 1954

GROUP 1
Excluded from automatic downgrading and declassification

CLASSIFIED DOCUMENT—TITLE UNCLASSIFIED

This material contains information affecting the national defense of the United States within the meaning of the espionage laws, Title 18, U.S.C., Secs. 793 and 794, the transmission or revelation of which in any manner to an unauthorized person is prohibited by law.

NOTICE

This document should not be returned after it has satisfied your requirements. It may be disposed of in accordance with your local security regulations or the appropriate provisions of the Industrial Security Manual for Safe-Guarding Classified Information.

NATIONAL AERONAUTICS AND SPACE ADMINISTRATION

[redacted]

[redacted]

AXIAL-POWER-DISTRIBUTION OPTIMIZATION IN THE TUNGSTEN WATER-MODERATED REACTOR (U)

by Edward Lantz

Lewis Research Center

SUMMARY

For the comparatively large temperature differences obtained in nuclear rocket reactors, a significant savings in core length can be obtained by tailoring the axial-power distribution so that as much of the core as possible is operating at the maximum allowable temperature. An optimumly zoned core can be from 25 to 30 percent shorter than an unzoned core and still produce the same outlet gas temperature for a given maximum fuel surface temperature.

A shorter core will result in less friction pressure drop for the propellant hydrogen. Also, since the reactor is the heaviest component of the rocket engine, a 25 percent shorter core would mean a significant increase in thrust-to-weight ratio and a consequent increase in rocket payload.

Attaining this savings in core length, however, requires finding the exact power distribution for a given temperature distribution. This determination is, in general, a problem which requires an iterative-type solution, and, as a consequence, the perturbation method described herein can reduce the required number of iterations and can ensure that the greatest possible savings in core length is obtained.

It is also shown that in order to get the desired power distribution in the tungsten water-moderated rocket reactor, both a good inlet end neutron reflector and an axially nonuniform core composition, such as varying fuel or parasitic absorber density, are required.

INTRODUCTION

According to Newton's law of cooling, more power can generally be transferred from a hot solid surface to a cold gas than to a hot gas. As a consequence, in a solid-core nuclear rocket, where a hydrogen propellant is heated to the highest possible temperature with a limited maximum solid fuel temperature, more power can be transferred to the propellant at the inlet end where the propellant is cool than at the exit end where the propellant is hot and is approaching the fuel-element surface temperature. Thus, in order to make the

[redacted]

most effective use of the heat-transfer area in the reactor, more power should be generated in the inlet half of the reactor than in the exit half. This requires an inlet end neutron reflector and a core which is of a nonuniform composition in the axial direction.

The advantage of tailoring the axial-power distribution in a gas-cooled reactor was noted in the aircraft nuclear propulsion program (ref. 1) and was also recognized in the design of the ML-1 reactor (ref. 2). However, the temperature difference between the fuel surface and the coolant gas at the inlet end of these cores is considerably smaller than that of rocket cores, and since the heat-transfer-area savings that can be obtained by axial-power tailoring is a direct function of this temperature difference, only comparatively small savings in heat-transfer areas were obtained in these two cases. A qualitative description of the increased heat-transfer effectiveness thus obtained in a rocket core and a brief description of a heterogeneous tungsten rocket reactor are given in reference 3. The axially tailored power example in reference 3 did not have the maximum allowable fuel surface temperature throughout the reactor. This temperature is required for maximum heat transfer from a given heat-transfer area.

The calculation of the axial-power distribution in a single average flow passage of a reactor which has the maximum allowable fuel surface temperature over its whole length is a complex problem. The heat-transfer coefficient between the fuel elements and the hydrogen propellant is primarily a function of fuel surface temperature, hydrogen temperature, and hydrogen velocity. The temperatures and velocity are, in turn, dependent on the heat-transfer coefficient. Because of these interactions, an open-form solution is generally required.

The axial-temperature distributions have not been optimized in the present generation of rocket reactors. At the power densities of these cores, small errors in the required power density can lead to a comparatively large deviation in temperature; thus an orderly approach is needed to predict the power distribution for a given temperature distribution. In order to eliminate some of the iterations in the optimization procedure, the following perturbation procedure was devised.

HEAT TRANSFER ANALYSIS, CALCULATIONS, AND RESULTS

For a given propellant gas inlet and outlet temperature and a given maximum surface temperature, the minimum heat-transfer length of an axial-flow channel is obtained when the entire length is maintained at the maximum surface temperature. This is evident from equation (A9) of appendix A, that is,

$$T_s(\Delta z) - T_g(\Delta z) = \frac{q(z)a}{h} \tag{1}$$

(All symbols are defined in appendix B.) Thus it is seen that the maximum power is obtained at each axial point with a maximum surface temperature. However, there are a number of considerations that may force a decreased surface temperature at the inlet end of the core. With the procedure to be described here, one can start with an allowable axial fuel-plate surface-temperature distribution,

which comes as close as possible to having the fuel plate surface temperature a maximum throughout the length of the flow channel, and derive the required axial-power distribution to attain this surface-temperature distribution.

The two basic equations, which are equations (A6) and (A9) of appendix A, are

$$T_g(\Delta z) = \frac{A_{xy}}{\dot{M}C_p} \int_{z=0}^{z=\Delta z} q(z)dz + (T_g)_i \tag{2}$$

$$T_s(\Delta z) = T_g(\Delta z) + \frac{q(z)a}{h} \tag{3}$$

The method is to divide an average flow channel of the reactor into a sufficient number of axial nodes of length Δz such that for each axial node, n

$$q(z) \equiv q_n, \text{ a constant of node } n \tag{4}$$

$$\frac{A_{xy}}{\dot{M}C_p} \equiv (C_1)_n, \text{ a constant of node } n \tag{5}$$

$$\frac{a}{h} \equiv (C_2)_n, \text{ a constant of node } n \tag{6}$$

Then from equations (2), (4), and (5) for any successive node, n

$$(T_g)_n = (C_1)_n q_n \Delta z + (T_g)_{n-1} \tag{7}$$

where

$$(T_g)_i = (T_g)_{n-1}$$

that is, the gas temperature at the inlet of a node is equal to the gas temperature at the outlet of the preceding node. Solving equation (7) for $(C_1)_n$ gives

$$(C_1)_n = \frac{(T_g)_n - (T_g)_{n-1}}{q_n \Delta z} \tag{8}$$

Also, from equations (3) and (6),

$$(T_s)_n = (T_g)_n + (C_2)_n q_n \tag{9}$$

Solving equation (9) for $(C_2)_n$ gives

$$(C_2)_n = \frac{(T_s)_n - (T_g)_n}{q_n} \tag{10}$$

Substituting for $(T_g)_n$ as given by equation (7) into equation (9) gives

$$(T_s)_n = (C_1)_n q_n \Delta z + (T_g)_{n-1} + (C_2)_n q_n$$

or,

$$q_n = \frac{(T_s)_n - (T_g)_{n-1}}{(C_1)_n \Delta z + (C_2)_n} \tag{11}$$

Now the procedure is to assume an initial power distribution for a calculation by a heat-transfer program which solves, as rigorously as possible, for the gas-temperature distribution $T_g(z)$ and the surface temperature distribution $T_s(z)$. With these temperatures used in conjunction with the input power distribution, the nodal constants $(C_1)_n$ and $(C_2)_n$ can be determined for each axial node from equations (8) and (10). Nodal constant $(C_2)_n$ will now have a total heat-transfer coefficient in it which includes radiation as well as convection. A sample of the results of this calculation, which is based on a typical temperature distribution, is shown in table I. One can now use this set of constants to calculate the required power distribution for a desired temperature distribution. This calculation can be made by first breaking the temperature distribution into the same nodes for which the constants were calculated and then solving equations (11) and (7) successively[1] for the nodal power densities. A sample of the results of this calculation is given in table II.

---

[1]With $n = 1$ equation (11) is

$$q_1 = \frac{(T_s)_1 - (T_g)_0}{(C_1)_1 \Delta z + (C_2)_1}$$

Then from equation (7)

$$(T_g)_1 = (C_1)_1 q_1 \Delta z + (T_g)_0$$

Therefore for $n = 2$,

$$q_2 = \frac{(T_s)_2 - (T_g)_1}{(C_1)_2 \Delta z + (C_2)_2}$$

etc. This process can be continued for all nodes.

The surface temperature distribution assumed for table II is flatter than that of table I. Thus, the power densities in the nodes closer to the inlet are higher and the resulting outlet gas temperature is higher for a given maximum surface temperature.

In order to check the perturbation method, the power distribution calculated in table II and plotted in figure 1 was put into the rigorous heat-transfer program and the temperatures recalculated. The results of this calculation are given in table III. When the hand calculated temperatures of table II are compared with the rigorously calculated ones of table III, some differences can be seen. However, the method is sufficiently accurate to be of value in determining the required power distribution for a given temperature distribution.

The gas-temperature distribution given in table III was for a single flow channel, which was not quite the average channel. The gas temperature at the outlet of the average channel is 2478° K, rather than 2572° K. Also, the temperature distribution of table III was calculated with a value of heat-transfer coefficient that was too low for the nodes close to the inlet end. A better heat-transfer correlation has been determined by John V. Miller and Maynard F. Taylor (ref. 4). This correlation was used, and the calculations just described were redone to determine the optimized axial-power distribution shown in figure 2. This power distribution had a considerably flatter temperature distribution than that obtained from the power distribution of figure 1. This power distribution produces the same average gas temperature as before (i.e., 2478° K), but does it with a maximum surface temperature of 2640° K rather than the 2731° K obtained in table III. Thus for a given surface temperature, a higher gas temperature and specific impulse can be produced by an optimized power distribution. Alternatively, the same gas temperature can be obtained with a shorter core.

In order to evaluate the advantage of tailoring the axial-power distribution, a core heat-transfer efficiency ϵ can be defined as was done in reference 5:

$$\epsilon = \frac{(T_g)_e - (T_g)_0}{(T_s)_{max} - (T_g)_0} \tag{12}$$

For this analysis, $(T_g)_0 = 222^\circ$ K and $(T_g)_e = 2478^\circ$ K. The $(T_s)_{max}$ and ϵ for various axial-power distributions are listed in table IV. As is seen there, the heat-transfer efficiency can be increased from 0.83 for the unzoned, unreflected case to 0.93 for the optimum power distribution in the same length core. Alternatively, if the same $(T_s)_{max}$ is allowed in core 3 as in core 1, the core length can be reduced by 26 percent.

NEUTRONIC CONSIDERATIONS

The tungsten water-moderated reactor concept is briefly described in ref-

erence 3. The characteristic axial-power distribution of the unzoned, unreflected core is cosine shaped. Putting an approximately 7.5-centimeter, 70 percent beryllium - 30 percent water reflector on the inlet end changes the distribution to that shown in figure 3 and brings the heat-transfer efficiency up from 0.83 to 0.88 (see table IV).

One method for getting the desired power distribution is to vary the uranium 235 concentration in the axial direction. This can be seen from

$$q(z) \propto N_f \sigma_f \varphi(z) \tag{13}$$

Thus increasing N_f in the inlet end of the core increases $q(z)$ there. One of the disadvantages of this type of zoning is that in a practical zoned situation N_f is not a continuous function in the axial direction but rather a discontinuous function. Since $\varphi(z)$ is a continuous function, a discontinuous N_f causes a discontinuous $q(z)$ (i.e., power density). This is not an insurmountable problem but is an annoying one.

Another method of tailoring the power distribution is to add an axially varying amount of parasitic neutron absorber to the core. Thus, to obtain the zoned power distribution of figure 1, one would add a parasitic neutron absorber, such as natural tungsten in the tungsten water-moderated reactor, in the exit half of the core. This type of zoning varies $\varphi(z)$ rather than N_f, and $\varphi(z)$ is always a continuous function; so that in this type of zoning the power distribution is continuous.

In both the fuel and parasitic absorber zoning, a loss in core reactivity (i.e., neutron multiplication factor) is sustained. In the fuel zoning, the reactivity is lost because the metallurgically allowable maximum fuel concentration can no longer be used throughout the full volume of the core. In parasitic-absorber-zoning, neutrons that were captured by the fissioning fuel in the unzoned core are captured by the parasitic absorber in the zoned core. In obtaining the power distribution of figure 1 by either fuel or parasitic absorber zoning, about 4 percent in reactivity is lost. In obtaining the power distribution of figure 2, an 8.5 percent loss in reactivity is sustained. A conceivable way of obtaining the power distribution of figure 2 while keeping the reactivity loss to a minimum is to make use of a fueled inlet end reflector with materials such as beryllium oxide and uranium dioxide.

SUMMARY OF RESULTS

The following results were obtained from this study of the axial-power distribution in a hydrogen-cooled solid-core nuclear rocket reactor:

1. The perturbation method described here can be used to reduce the required number of iterations between power distribution and temperature distribution and thus help to ensure that the desired temperature distribution is obtained.

2. A significant savings in core length can be obtained by tailoring the

[redacted]

cosine-shaped axial-power distribution of a rocket reactor. A savings of at least 26 percent can be obtained in the tungsten water-moderated reactor by using an axially zoned distribution which costs about 4 percent in core reactivity. A greater savings can be obtained if more reactivity could be afforded for this purpose or if a beryllium oxide - uranium dioxide inlet end reflector is used.

Lewis Research Center,
National Aeronautics and Space Administration,
Cleveland, Ohio, November 23, 1965.

[redacted]

[redacted]

APPENDIX A

GENERAL HEAT-TRANSFER EQUATIONS

Expressions for surface and gas temperatures in a solid-fuel heat-exchange reactor in a steady-state condition are derived as follows:

The power generation dQ in an elemental volume at an axial point z is given by

$$dQ = q(z)A_{xy}\,dz,\ W \tag{A1}$$

where

$q(z)$ average power density in elemental volume, W/cm^3

A_{xy} fuel area in x,y-plane, which is transverse to the z-direction, cm^2

dz axial length of elemental volume, cm

With respect to energy conservation for a steady-state condition, the power generation in the elemental volume is also given by

$$dQ = \dot{M}C_p\,dT_g,\ W \tag{A2}$$

where

$\dot{M}$ propellant mass flow, kg/sec

C_p specific heat of propellant, $J/(kg)(^oK)$

and

$$dT_g = T_g(\Delta z) - (T_g)_i \tag{A3}$$

where

$T_g(\Delta z)$ propellant gas temperature at outlet end of elemental volume, ^oK

$(T_g)_i$ propellant gas temperature at inlet end of elemental volume, ^oK

From equations (A1) and (A2),

$$q(z)A_{xy}\,dz = \dot{M}C_p\,dT_g \tag{A4}$$

Integrating both sides of equation (A4) over an axial node of length Δz gives

$$T_g(\Delta z) - (T_g)_i = \frac{A_{xy}}{\dot{M}C_p}\int_{z=0}^{z=\Delta z} q(z)dz \tag{A5}$$

[redacted]

[redacted]

where the node length is so chosen that C_p is essentially constant. Thus, dT_g is proportional to the integral of the power density or total power, and the gas temperature at a node outlet is

$$T_g(\Delta z) = \frac{A_{xy}}{\dot{M}C_p} \int_{z=0}^{z=\Delta z} q(z)dz + (T_g)_i \qquad \text{(A6)}$$

Also applying Newton's law of cooling at an axial point z at the outlet of a node gives

$$q(z)aA_{HT} = hA_{HT}\left[T_s(\Delta z) - T_g(\Delta z)\right] \qquad \text{(A7)}$$

where

a fuel-plate thickness, cm

A_{HT} nodal heat-transfer area, cm^2

h heat-transfer coefficient to gas, $W/(cm^2)(^oK)$

$T_s(\Delta z)$ fuel-plate surface temperature at node outlet, ^oK

$T_g(\Delta z)$ gas temperature at node outlet, ^oK

Simplifying equation (A7) gives

$$T_s(\Delta z) - T_g(\Delta z) = \frac{q(z)a}{h} \qquad \text{(A8)}$$

or

$$T_s(\Delta z) = T_g(\Delta z) + \frac{q(z)a}{h} \qquad \text{(A9)}$$

Substituting for $T_g(\Delta z)$ as expressed in equation (A6) into equation (A9) gives

$$T_s(\Delta z) = \frac{A_{xy}}{\dot{M}C_p} \int_{z=0}^{z=\Delta z} q(z)dz + (T_g)_i + \frac{q(z)a}{h} \qquad \text{(A10)}$$

[redacted]

APPENDIX B

SYMBOLS

A_{xy}	fuel area in x,y-plane, which is transverse to z-direction, cm^2
a	fuel-plate thickness, cm
C_p	specific heat of propellant at constant pressure, $J/(kg)(^oK)$
$(C_1)_n$	heat capacity constant of node n, $(^oK)(cm^2)/W$, eq. (5)
$(C_2)_n$	heat-transfer constant of node n, $(^oK)(cm^3)/W$, eq. (6)
h	heat-transfer coefficient to gas, $W/(cm^2)(^oK)$
$\dot{M}$	propellant mass flow, kg/sec
N_f	atom density of fuel, $atoms/cm^3$
n	axial node
q(z)	average power density in elemental volume, W/cm^3
q_{av}	average power density of all axial nodes, W/cm^3
q_n	average power density in node n, W/cm^3
T_g	gas temperature, ^oK
$(T_g)_e$	gas temperature at final node, ^oK
$(T_g)_i$	gas temperature at inlet of node, ^oK
$(T_g)_n$	gas temperature at outlet of node, ^oK
$(T_g)_0$	gas temperature at inlet to first axial node, ^oK
$T_g(\Delta z)$	gas temperature at node outlet, ^oK
$T_{s,max}$	maximum surface temperature in core, ^oK
$(T_s)_n$	surface temperature of node, ^oK
$T_s(\Delta z)$	fuel-plate surface temperature at node outlet, ^oK
ϵ	core heat-transfer efficiency
σ_f	fission cross section for neutrons, cm^2
$\varphi(z)$	neutron flux at axial point z, $neutrons/(cm^2)(sec)$

[redacted]

REFERENCES

1. Thornton, Gunnar; and Blumberg, Ben: ANP HTREs Fulfill Test Goals. Nucleonics, vol. 19, no. 1, Jan. 1961, pp. 45-51.

2. Egen, Richard A.; Hogan, William S.; Dingee, David A.; and Chastain, Joel W.: ML-1-1A Core Studies With the GCRE Critical Assembly. Rep. No. BMI-1396, Battelle Memorial Institute, Nov. 27, 1959.

3. Bogart, Donald; and Lantz, Edward: Nuclear Physics of Solid-Core Gas-Cooled Rocket Propulsion Reactors. Proceedings of the NASA-University Conference on the Science and Technology of Space Exploration, vol. 2, NASA SP-11, 1962, pp. 77-86. (Also available as NASA SP-20.)

4. Miller, John V.; and Taylor, Maynard F.: Improved Method of Predicting Surface Temperatures in Hydrogen-Cooled Nuclear Rocket Reactor at High Surface- to Bulk-Temperature Ratios, NASA TN D-2594, 1965.

5. Advanced Rocket Reactor Technology Group: Nuclear Rocket Study Evaluation Report. Rept. No. ANL-JFM-10, Argonne Nat. Lab., Dec. 1962, pp. 120-122.

[redacted]

[redacted]

TABLE I. - NODAL CONSTANTS C_1 AND C_2 FROM INITIAL HEAT-TRANSFER CALCULATION

[$q_n \equiv$ Average power density of node n; $q_{av} \equiv$ average power density over all axial nodes;

$$(C_1)_n \Delta z = \frac{(T_g)_n - (T_g)_{n-1}}{q_n/q_{av}}; \quad (C_2)_n = \frac{(T_s)_n - (T_g)_n}{q_n/q_{av}}.]$$

Axial node, n	q_n/q_{av}	$(T_g)_n - (T_g)_{n-1}$, °K	$(T_s)_n - (T_g)_n$, °K	$(C_1)_n \Delta z$	$(C_2)_n$
1	0.81	167	1056	206.17	1303.70
2	.96	195	1007	203.13	1048.96
3	1.08	195	960	180.56	888.89
4	1.15	195	916	169.57	796.52
5	1.19	195	868	163.87	729.41
6	1.20	208	822	173.33	685.00
7	1.15	180	739	156.52	642.61
8	1.11	195	667	175.68	600.90
9	1.06	139	598	131.13	564.15
10	1.01	153	539	151.48	533.66
11	.97	158	483	162.89	497.94
12	.89	133	429	149.44	482.02
13	.81	111	368	137.04	454.32
14	.61	73	244	119.67	400.00

TABLE II. - CALCULATED NODAL POWER DENSITIES q'_n/q_{av} FOR ASSUMED SURFACE TEMPERATURE $(T_s)_n$

$$\left[\frac{q'_n}{q_{av}} = \frac{(T_s)_n - (T_g)_{n-1}}{(C_1)_n \Delta z + (C_2)_n}; \quad (T_g)_n = (C_1)_n \left(\frac{q'_n}{q_{av}}\right) \Delta z + (T_g)_{n-1}.\right]$$

Axial node, n	$(T_s)_n$, °K	$(C_1)_n \Delta z + (C_2)_n$	$\frac{q'_n}{q_{av}}$	$(C_1)_n \Delta z \frac{q'_n}{q_{av}}$	$(T_g)_n$, °K
0	----	-------	----	------	222
1	1656	1509.87	0.95	195.86	418
2	1921	1252.09	1.20	243.76	662
3	2084	1069.45	1.33	240.14	902
4	2245	966.09	1.39	235.70	1138
5	2379	893.28	1.39	227.78	1366
6	2482	858.33	1.30	225.33	1591
7	2550	799.13	1.20	187.82	1779
8	2633	776.58	1.10	193.25	1972
9	2667	695.28	1.00	131.13	2103
10	2699	685.14	.87	131.79	2235
11	2730	660.83	.75	122.17	2357
12	2735	631.46	.60	89.66	2447
13	2754	591.36	.52	71.26	2518
14	2726	519.67	.40	47.87	2566

[redacted]

[redacted]

TABLE III. - COMPUTER CALCULATED TEMPERATURES FOR PERTURBED POWER DISTRIBUTION q'_n/q_{av}

Axial node, n	q'_n/q_{av}	$(T_g)_n$, °K	$(T_s)_n$, °K
0	----	222	----
1	0.95	432	1626
2	1.20	657	1877
3	1.33	903	2043
4	1.39	1153	2210
5	1.39	1393	2356
6	1.30	1610	2436
7	1.20	1804	2499
8	1.10	1978	2568
9	1.00	2131	2633
10	.87	2260	2671
11	.75	2368	2703
12	.60	2451	2705
13	.52	2521	2731
14	.40	2572	2724

TABLE IV. - HEAT-TRANSFER EFFICIENCIES ϵ FOR CORES WITH VARYING DEGREES OF AXIAL-POWER TAILORING

[Gas inlet and outlet temperatures, 222° and 2478° K, respectively.]

Core	Axial-power distribution	Maximum surface temperature, °K	Heat-transfer efficiency, ϵ
1	Unzoned, unreflected	2944	0.83
2	Reflected, unzoned	2800	.88
3	Zoned power distribution (fig. 1)	2731	.90
4	Optimum power distribution (fig. 2)	2640	.93

[redacted]

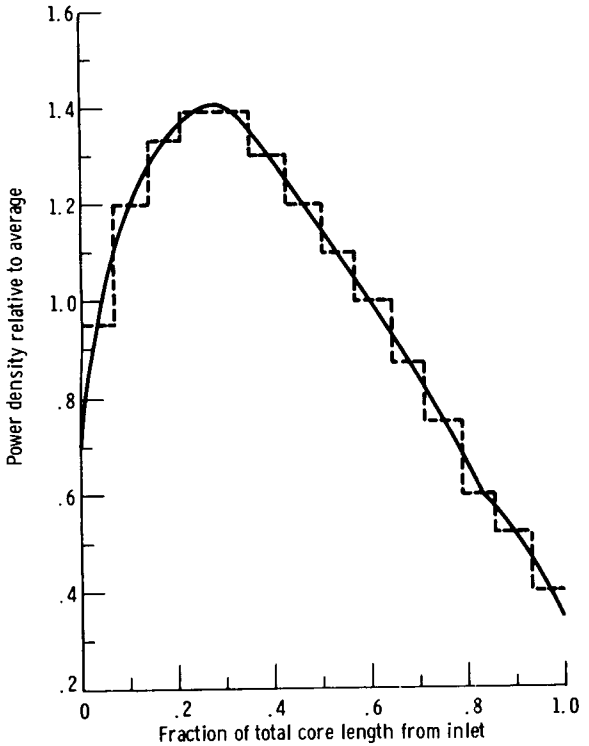

Figure 1. - Axial-power distribution for temperature distribution of table III.

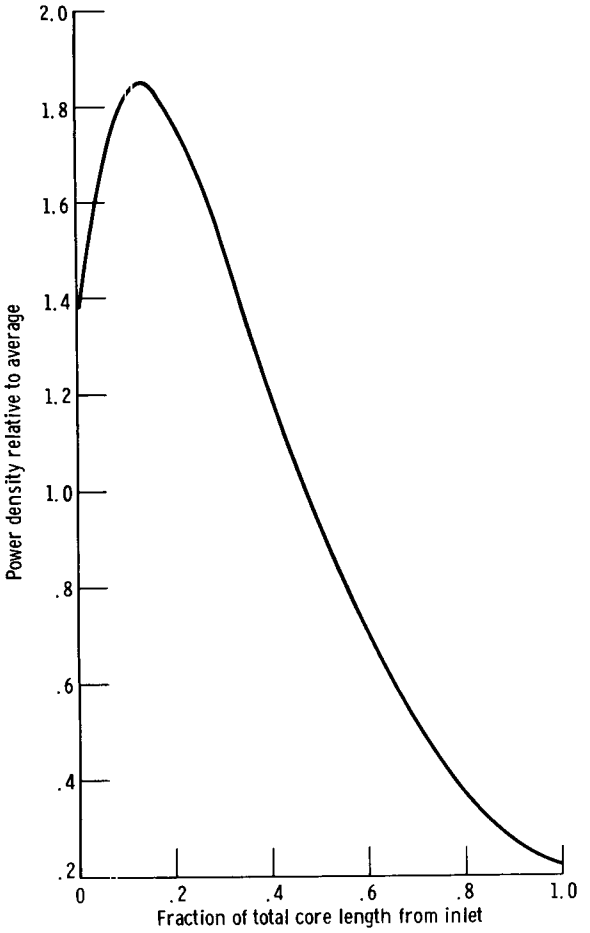

Figure 2. - Optimum axial-power distribution.

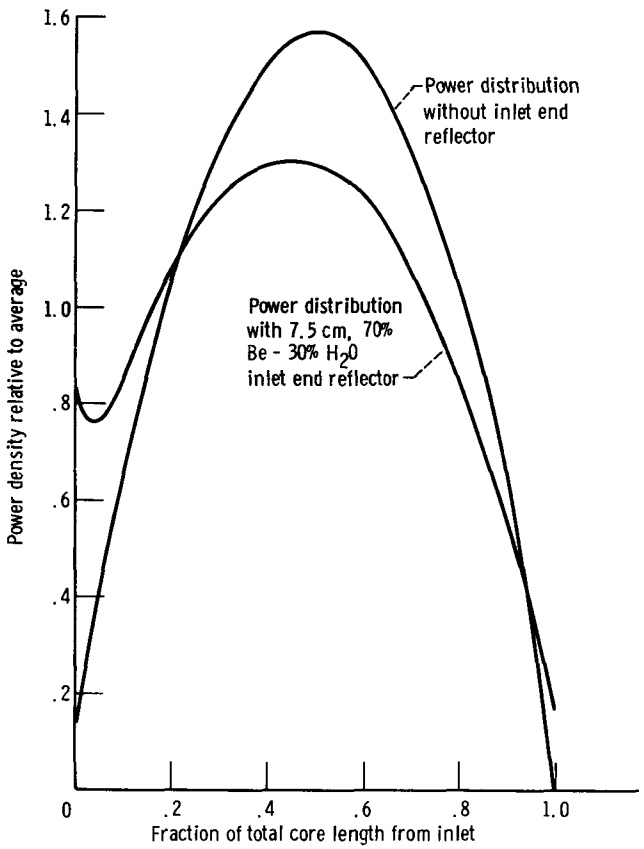

Figure 3. - Comparison of axial-power distribution of tungsten water-moderated reactor with and without inlet end reflector.

[redacted]

"The aeronautical and space activities of the United States shall be conducted so as to contribute . . . to the expansion of human knowledge of phenomena in the atmosphere and space. The Administration shall provide for the widest practicable and appropriate dissemination of information concerning its activities and the results thereof."

—NATIONAL AERONAUTICS AND SPACE ACT OF 1958

NASA SCIENTIFIC AND TECHNICAL PUBLICATIONS

TECHNICAL REPORTS: Scientific and technical information considered important, complete, and a lasting contribution to existing knowledge.

TECHNICAL NOTES: Information less broad in scope but nevertheless of importance as a contribution to existing knowledge.

TECHNICAL MEMORANDUMS: Information receiving limited distribution because of preliminary data, security classification, or other reasons.

CONTRACTOR REPORTS: Technical information generated in connection with a NASA contract or grant and released under NASA auspices.

TECHNICAL TRANSLATIONS: Information published in a foreign language considered to merit NASA distribution in English.

TECHNICAL REPRINTS: Information derived from NASA activities and initially published in the form of journal articles.

SPECIAL PUBLICATIONS: Information derived from or of value to NASA activities but not necessarily reporting the results of individual NASA-programmed scientific efforts. Publications include conference proceedings, monographs, data compilations, handbooks, sourcebooks, and special bibliographies.

Details on the availability of these publications may be obtained from:

SCIENTIFIC AND TECHNICAL INFORMATION DIVISION

NATIONAL AERONAUTICS AND SPACE ADMINISTRATION

Washington, D.C. 20546

[redacted]